The effect of a subcutaneous silicone rubber implant with shallow surface microgrooves on the surrounding tissues in rabbits

E. T. den Braber, J. E. de Ruijter, J. A. Jansen
University of Nijmegen, Dental School, Laboratory of Biomaterials, POB 9101, 6500 HB Nijmegen, The Netherlands

Received: 20 November 1996; accepted 13 December 1996

Abstract: It has been suggested that during wound healing microtextured surfaces can alter events at the interface between implant surface surface and surrounding tissues. To investigate this phenomenon, smooth and microtextured silicone rubber implants were implanted subcutaneously in rabbits for 3, 7, 42, and 84 days. The textured implants possessed parallel surface microgrooves and ridges with a width of 2.0, 5.0, and 10.0 μm. All grooves had a depth of approximately 0.5 μm. SEM observation showed fibroblasts, erythrocytes, lymphocytes, macrophages, fibrin, and collagen on all implant surfaces after 3 and 7 days. After 42 and 84 days only little collagen, a small number of fibroblasts, but no inflammatory cells were seen on the implant surfaces. The fibroblasts were not oriented along the surface grooves on all textured surfaces. Three-dimensional reconstruction of CLSM images and LM images showed no significant differences between the thickness of the capsules surrounding the smooth and those surrounding the microgrooved implants. In contrast, LM did show a significantly lower number of inflammatory cells and a significantly higher number of blood vessels in the capsules surrounding the microgrooved implants. Differences between the 2.0, 5.0, and 10.0 μm grooved implants were not detected. Our results concerning the capsule thickness suggest that the depth of our grooves was not sufficient to facilitate mechanical interlocking, but the cause for the observed differences in inflammatory response and number of blood vessels remains unclear.
 J Biomed Mater Res, 37, 539–547, 1997.

Key words: *in vivo;* soft-tissue reaction; scanning electron microscopy; confocal laser scanning microscopy; three-dimensional *reconstruction; implant interface*

INTRODUCTION

The interaction between an implant material and the surrounding tissues can be considered vital for the final clinical performance of implanted artificial medical devices. For example, the promotion of tissue attachment and the concomitant reduction of the highly undesirable chronic inflammatory response and fibrosis around implant materials are of central importance for the biocompatibility of biomaterials.[1] Since various surface properties[2] of an implant material determine the biocompatibility of these materials, surface modifications based on the most recent technologies are being explored in search of the ideal implant surface.[3] This study will focus on one of these modifications, i.e. implant surface texturing on a micrometer scale.

Earlier studies have shown that microgeometrical patterns on substratum surfaces have a high potential for provoking specific cellular reactions by influencing basic cellular mechanisms, such as DNA/RNA-related processes, cellular attachment, and cell locomotion.[1,2] This led to the idea that surface microtexturing could be used deliberately to achieve certain desired end results in processes such as morphogenesis, cell invasion, repair, and regeneration.[4] If this hypothesis proves to be true, it is obvious that surface texturing can be a very important tool in designing successful implants.[1,4] Unfortunately, most of the currently available information on microtextured-related cellular behavior is derived from *in vitro* experiments. *In vivo* studies with microtextured implants are scarce. Moreover, review of these *in vivo* studies shows that the design of the textured implants used is very diverse. But even with this large diversity of design, the potential of microtextured implant surfaces impacting several implant-related processes can be perceived. For example, some studies,[5,6] have reported on the reduction of epithelial downgrowth with microgrooved skin-penetrating devices. Other investigators, who implanted microporous or pillared surfaces subcutaneously, found tightly adherent fibrous capsules

Correspondence to: E. den Braber, e-mail address: E.denBraber@dent.kun.nl
Contract grant sponsor: Dutch Technology Foundation (STW)

 CCC 0021-9304/97/040539-09

without inflammatory cells,[7] reduced fibrosis,[8] and improved blood vessel proximity.[8] These results, together with the fact that our laboratory has been involved in the development of a new subcutaneously anchored percutaneous device for more than 10 years,[9–13] suggested a study of tissue response using standardized surface patterns. The specific aim of this study was to evaluate the effect of a subcutaneous implant with a standardized pattern of shallow surface microgrooves on the surrounding tissues in rabbits.

MATERIALS AND METHODS

Production and characterization of the microtextured substrata

Surface-textured experimental substrata were produced by first making silicon oxide molds with photolithography.[14,15] These molds were covered with silicone elastomer (MDX 4-4210, Dow Corning), and after polymerization the silicone rubber surface replica was removed from the mold. The final experimental implants were obtained by cutting the silicone rubber castings into round disks. All implants had a diameter of 15.0 mm, were 1.45-mm thick, and had one smooth and one textured side. Subsequently, the implants were cleaned as described before[16] and prepared for implantation by radio frequency glow discharge (RFGD, PDC-3XG, Harrick; Argon, 0.15 Torr, 5 min). After RFGD treatment the implants were stored in sterile 6-well cell culture plates (Greiner) for transport to the operation theater.

Additional implants were produced to enable surface characterization. The production process and postproduction treatment of these implants were identical to those produced for implantation. The geometrical surface properties and the surface quality of the implants were investigated by scanning electron microscopy (SEM, JEOL 6310) and atomic force microscope (AFM, Polaron SP300). The designer dimensions of the surface pattern can be found in Table I.

Animal model and implantation

For implantation, a total of 12 female New Zealand White rabbits, 3 months of age (2–6 kg), were used. The smooth and textured implants were inserted for periods of 3, 7, 42, and 84 days (Fig. 1) and were placed in four separate surgical sessions, set up according to the split-plot design.[17] During every surgical session, the implants were placed on either the left or right side of the spinal column, enabling the evaluation of two implantation periods within a single rabbit. Randomization of the site of implantation for the various types of implant texture and length of implantation period was achieved with a Latin square implantation schedule (Fig. 1). For every period of implantation, six implants with an identical surface texture were used. In total, 96 implants were evaluated during this study.

Before surgery, the skin was shaved, washed, and disinfected with iodine. The actual surgical procedures were performed under general anesthesia induced by intramuscular injection of Hypnorm™ (0.5 mL/kg) and atropine (0.5 mg/animal). After orotracheal intubation, anesthesia was maintained by ethrane (2.0–3.0%) through a constant volume ventilator. During each surgical session, four paravertebral incisions of approximately 15 mm were made. Lateral to these incisions small subcutaneous pockets were created by blunt dissection with scissors. The implants

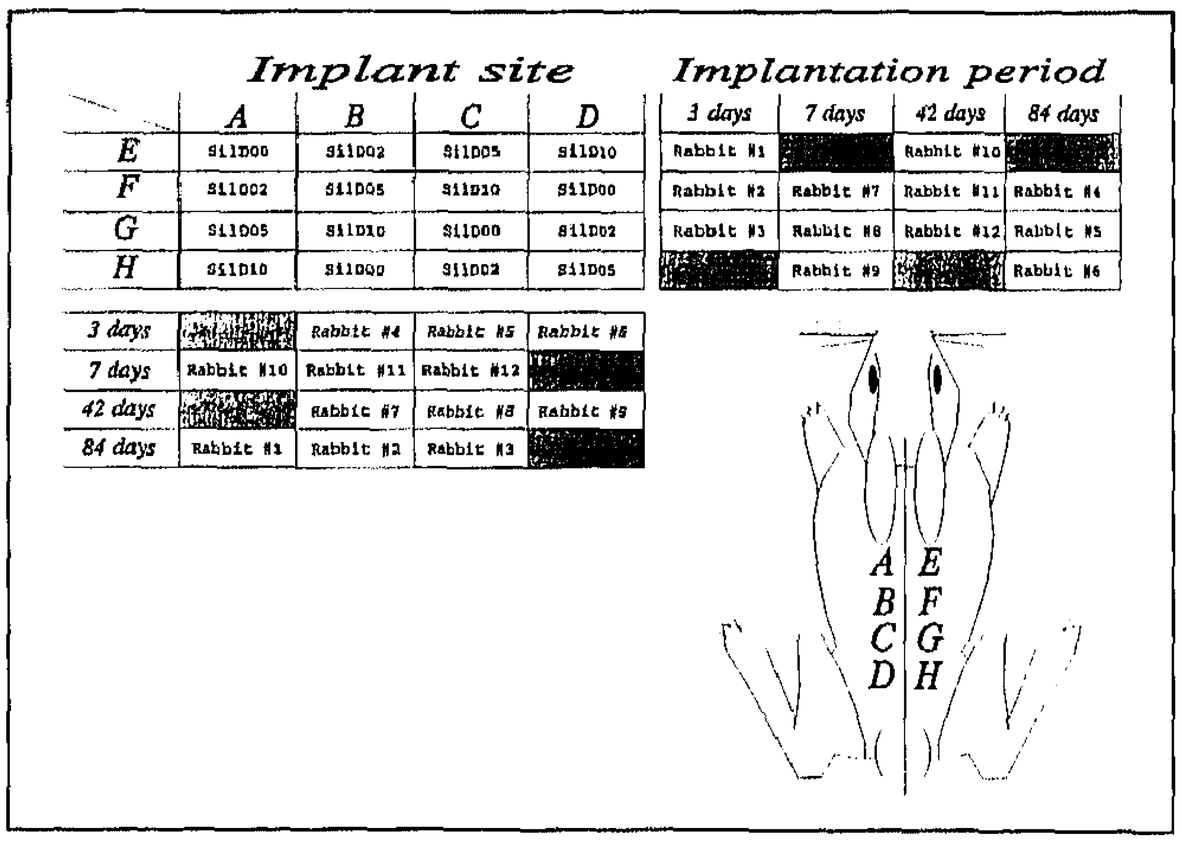

Figure 1. Schematic drawing of the rabbit shows the sites of implantation. The letters of these sites (A to D and E to H) correspond with the letters in the upper left hand table. This table, together with the two additional tables, makes it possible to determine which implant (smooth or textured) was implanted at which specific site. For example, the implantation periods for rabbit #8 were 7 (top right hand table) and 42 (bottom table) days. During the 7-day period, the SilD10 implant was located on site B and the SilD02 implant on site D (read upper left hand table from left to right) while during the 42-day period the SilD00 implant was located at site G (read upper left hand table from top to bottom). The implant names are given in Table I.

TABLE I
Designer Values of the Microgrooves on the Silicone Mold Surface

Surface	Designer Values			
	Gd (μm)	Gw (μm)	Rw (μm)	P (μm)
SilD00	—	—	—	—
SilD02	0.50	2.00	2.00	4.00
SilD05	0.50	5.00	5.00	10.00
SilD10	0.50	10.00	10.00	20.00

GD = groove depth; Gw = groove width; Rw = ridge idth; P = pitch.

were inserted into the pockets (textured side medial) but were not fixed with sutures. Finally, the wounds were closed intracutaneously with Vicryl™ 3-0. To reduce the perioperative infection risk, the prophylactic antibiotic Terramycine™ was administered postoperatively. After surgery, the animals were placed in a cage and allowed to move unrestricted at all times. Normal tap water and standard rabbit chow were provided *ad libitum*.

Histological evaluation

At the end of the implantation periods, the animals were killed with an overdose Nembutal™ (iv, 150 mg/kg). The skin was shaved and the implants with the surrounding tissues were excised immediately. A patch of tissue, containing one implant only, was labeled with a unique code, linking it directly to an implant with a specific surface texture, test animal, the date of removal, and the site of implantation. After fixing the specimens with 10% buffered formalin solution through immersion for 72 h, the tissue patch with the embedded implant was cut into two equal pieces. Subsequently, the implant became visible and was removed from the tissue capsule with tweezers. These removed halves of the silicone rubber implants were prepared for SEM examination, as described earlier.[18] In short, these samples were dehydrated by rinsing with 100% methanol for 5 min, air dried, sputter-coated with gold, and investigated by SEM (JEOL 6310).

After removal of the silicone implants, the tissue specimens were prepared for observation with confocal laser scanning microscopy (CLSM) and normal light microscopy (LM). The samples were dehydrated through a series of graded alcohol and Histoclear™ and embedded in Paraplast.™ Subsequently, 5.0 μm sections were cut with a Leitz microtome and stained with haematoxylin eosin (Mayer), Azan, May-Grünwald-Giemsa, trichrome (Goldner) and Picro-Sirius Red stains.[19] Since the Picro-Sirius Red stain exhibits autofluorescent properties when excited at λ = 568 nm, observation with a CLSM (Bio-Rad MRC 1000, Bio-Rad Laboratories) was possible. Subsequently, the Picro-Sirius Red sections were viewed with normal and oil objectives, mounted on a Nikon Diaphot microscope. Digital images were captured and stored, as described earlier,[20] and additional 3-dimensional reconstruction of the stained tissues was performed by using the Confocal Assistant V3.10 for Windows™ 3.1× program (available at FTP.GENETICS.BIO-RAD.COM, copyright Todd Clark Brelje, 1995).

In short, the histological assessment parameters for LM were: (1) the general appearance of the tissues surrounding the implant, (2) the presence and number of inflammatory cells, i.e. macrophages, giant cells, polymorphonuclear granulocytes (PMN), and plasma cells, and (3) the number and status of blood vessels in the surrounding fibrous capsule. For the analyses of

TABLE II
Parameters Used in the Statistical Analysis of the Soft-Tissue Microtextured Silicone Rubber Implants

GENERAL	[independent]
— Section#	[independent]
— Animal#	[L/R]
— Side	[1/2/3/4]
— Site	[3/7/42/84]
— Implantation period	[0/2/5/10]
— Implant texture	
CAPSULE, LOCALIZATION	
— No capsule present	[1]
— Capsule on 1 (dermis) side	[2]
— Capsule on 1 (medial) side	[3]
— Capsule on 2 sides present	[4]
CAPSULE, FORMATION	
— No capsule present	[1]
— Loose, fibro-elastic	[2]
— Loose, adipose	[3]
— Loose, fibro-adipose	[4]
— Less dense	[5]
— Dense	[6]
CAPSULE, CELLULAR	
— Fibroblast thickness	[1 = 0, 0 < 2 < 5, 5 < 3 < 10, 10 < 4 < 30, 5 > 30]
— Fibroblasts contacting surface	[1 = YES, 2 = NO]
— Acute/chronic inflam. process	[1 = AC, 2 = CHR]
— Severity inflammatory process	[1 = none, 4 = severe]
— Inflammatory cells location	[1 = non, 2 = end, 3 = middle, 4 = 2 + 3]
— Inflam. cells contacting surface	[1 = YES, 2 = NO]
— macrophages	[1 = YES, 2 = NO]
— giant cells	[1 = YES, 2 = NO]
— PMNs	[1 = YES, 2 = NO]
— plasma cells	[1 = YES, 2 = NO]
— Blood vessels present	[1 = YES, 2 = NO]
— mature/new vessels	[1 = MAT, 2 = NW]
CAPSULE SURROUNDING TISSUES	
— Acute/chronic inflam. process	[1 = AC, 2 = CHR]
— Severity inflammatory process	[1 = none, 4 = severe]
— macrophages	[1 = YES, 2 = NO]
— giant cells	[1 = YES, 2 = NO]
— PMNs	[1 = YES, 2 = NO]
— plasma cells	[1 = YES, 2 = NO]
— Blood vessels present	[1 = YES, 2 = NO]
— mature/new vessels	[1 = MAT, 2 = NW]

all the stained sections a refined histomorphometric grading scale[17,21] was used (Table II). Per examined section, the implant surrounding tissues were evaluated by gathering the scores of the histomorphometric parameters in Table II for 16 predetermined fields (Fig. 2). After scanning six sections of each implant, the results of the light microscopical evaluation were evaluated with SAS™ (release 6.03, SAS Institute Inc., USA), using univariate tests, Fisher Exact tests, and Spearman correlation models.

RESULTS

Macroscopic findings

Eight days after the start of the experiment, one of the 12 animals died due to pneumonia. This animal was replaced by a new rabbit, which received identical treatment and completed the initial implantation period. Except for this incident, all the experimental animals appeared to be in good health throughout the test period, and none of the rabbits had any wound complications. At sacrifice, all the silicone rubber implants were surrounded by a thin, reaction-free fibrous capsule. Macroscopically, there were no indications of differences in capsule thickness among the various implantation periods.

SEM observation of the excised implants

SEM examination revealed that, after an implantation period of 3 and 7 days, the surfaces of all the implants were covered with a dense layer. Fibroblasts proved to be embedded in this layer, while erythrocytes, lymphocytes, and macrophages were seen on top of this layer (Figs. 3 and 4). Furthermore, large quantities of fibrin (Fig. 4) and collagen (Fig. 5) were seen. The collagen fibers were located on top of the dense layer or directly in contact with the silicone surface. These fibers appeared to be oriented randomly on all textured surfaces.

After 42 and 84 days of implantation, only a few collagen fibers were observed on the surfaces of the retrieved silicone implants. On most of the implant surfaces only a dense deposit was visible. Occasionally fibroblasts were seen, but these cells did not show any signs of alignment with the surface pattern. As with the various textured implants after an implantation period of 3 and 7 days, no differences were found with regard to the number of cells or the amount of ECM material on the smooth and textured surfaces.

Descriptive LM and CLSM evaluation of the tissues surrounding the implant

Gross evaluation of the differently stained sections revealed that the tissue reaction to all implants appeared to be relatively uniform. After a 3-day implantation period, LM showed that the implants were surrounded by a loose collagen matrix containing fibroblasts and many inflammatory cells, i.e. granulocytes, macrophages, and monocytes (Fig. 6). At the interface between implant and the surrounding tissues, these inflammatory cells had accumulated while very few fibroblasts were seen at this location. In addition to the LM observation, 3-dimensional reconstruction of the loose collagen matrix surrounding the implants after 3

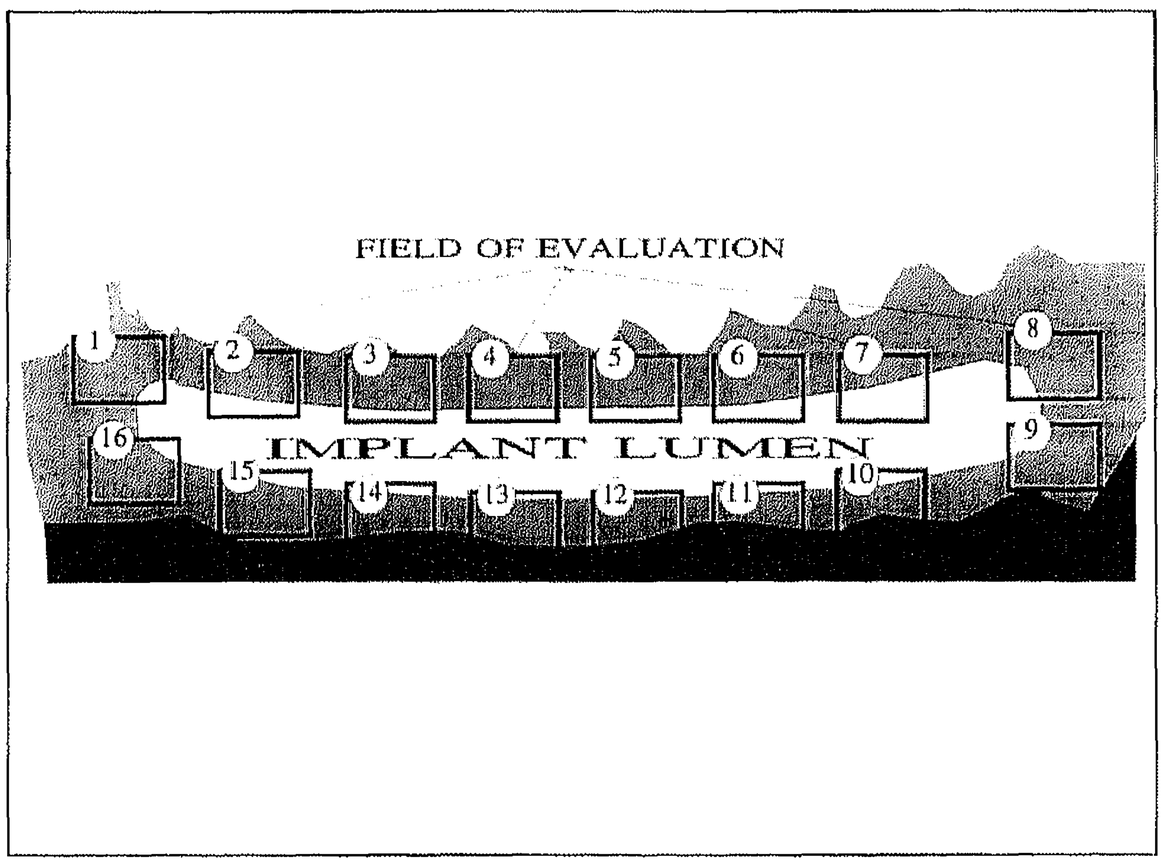

Figure 2. Schematic drawing representing a section. The implant lumen is clearly visible and the implant surrounding capsule is visualized with a lattice pattern. For histomorphometric evaluation a total of 16 evaluation areas were used.

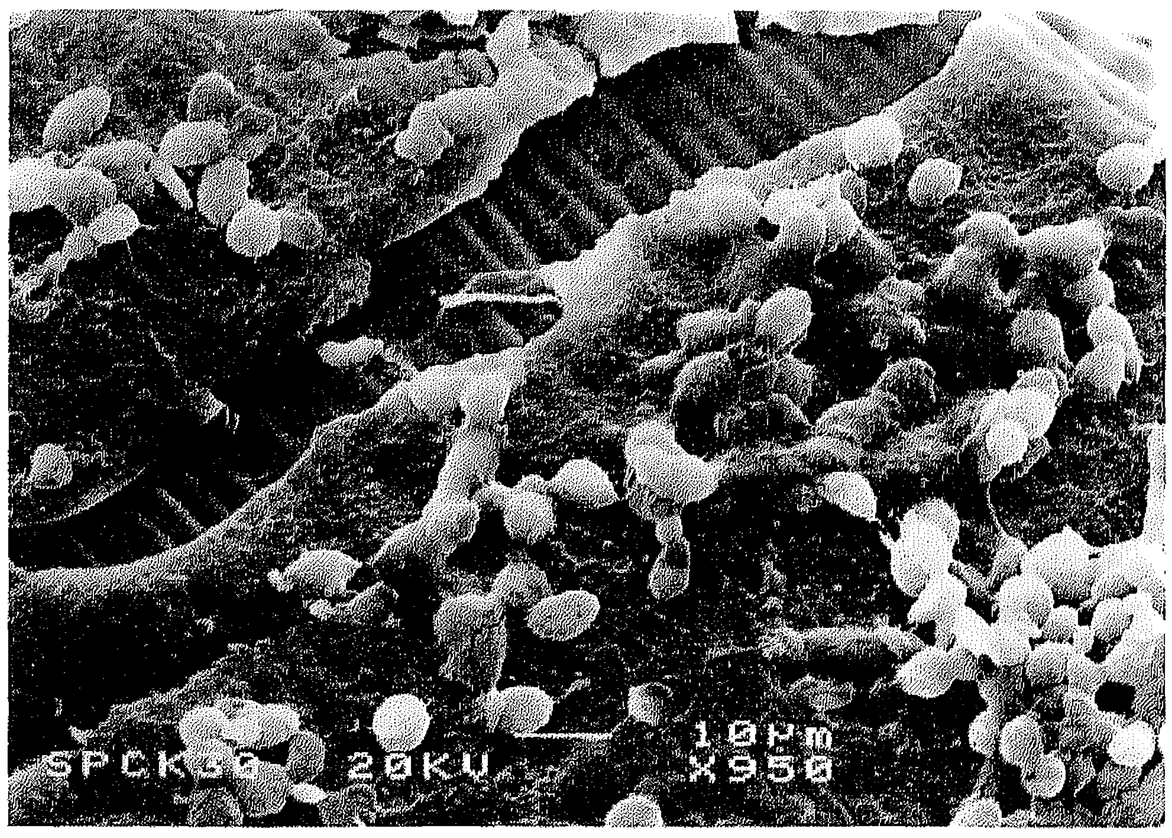

Figure 3. SEM micrograph of the surface of a 2.0 µm grooved implant after a 3-day implantation period. Underneath the dense layer with fibroblasts, the original grooved silicone surface is visible. On top of this layer erythrocytes and inflammatory cells can be seen.

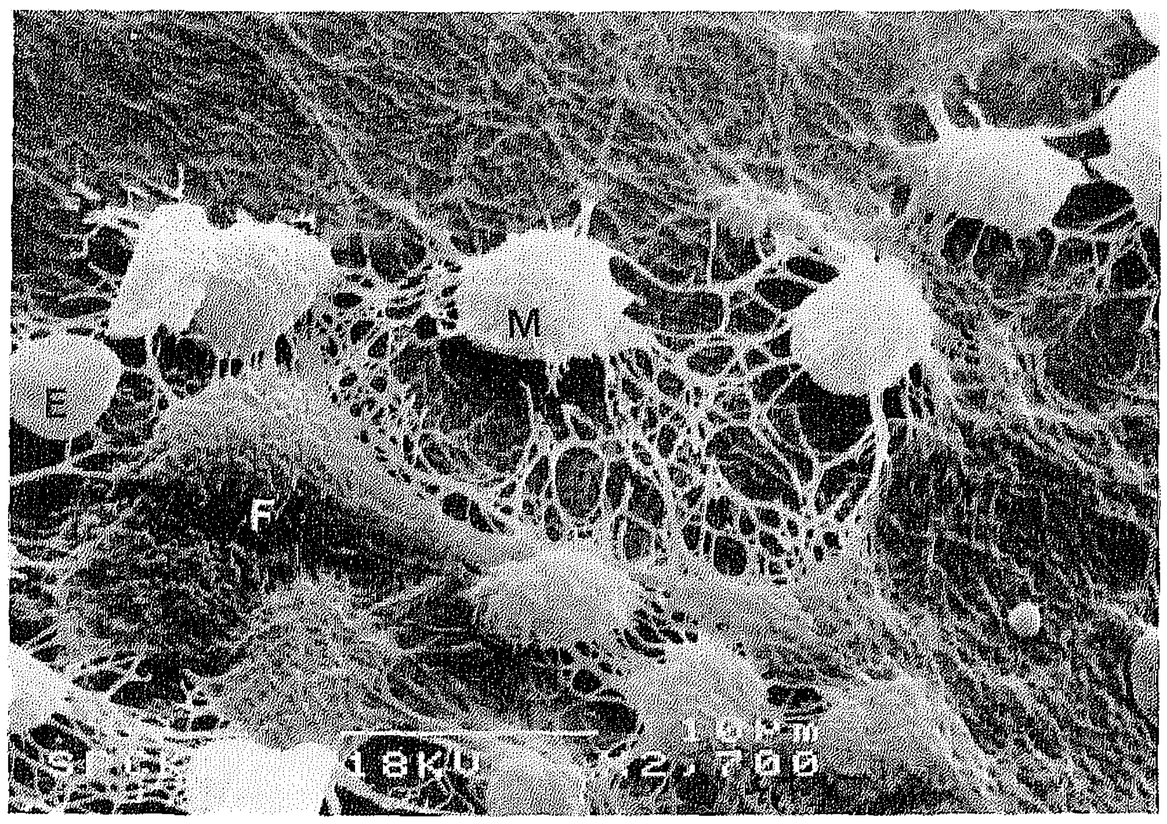

Figure 4. SEM image of 5.0 μm implant after 3 days of implantation. The silicone surface is totally covered and the surface grooves are not visible. Fibroblasts (F), macrophages (M), erythrocytes (E), and many fibrin fibers are present.

days revealed that very long collagen fibers were present, following the surface of the implant (Fig. 7). More or less perpendicular to these long fibers, smaller collagen fibers were seen forming a type of lattice. Finally, many globular structures were observed, which appeared to be attached to this loose collagen lattice.

CLSM observation of the tissues after an implantation period of 7 days showed a transition of the implant surrounding capsule from a loose collagen matrix to a more densely packed capsule. The collagen fibers in these capsules were much thicker. In addition, all the fibers seemed oriented parallel to the initial implant surface. LM investigation showed several layers of fibroblasts, which appeared as either active cells with a round nucleus or as highly elongated cells with a flattened nucleus. Very often these flat, elongated fibroblasts were found in or close to the surface layer of the tissues bordering the implant lumen. In addition, many sections showed newly formed vessels (Fig. 8). All the sections displayed a large decrease in the number of inflammatory cells. This decrease was seen most clearly at the interface between the tissues and the implant lumen, where no or few inflammatory cells were observed after 7 days (Fig. 9).

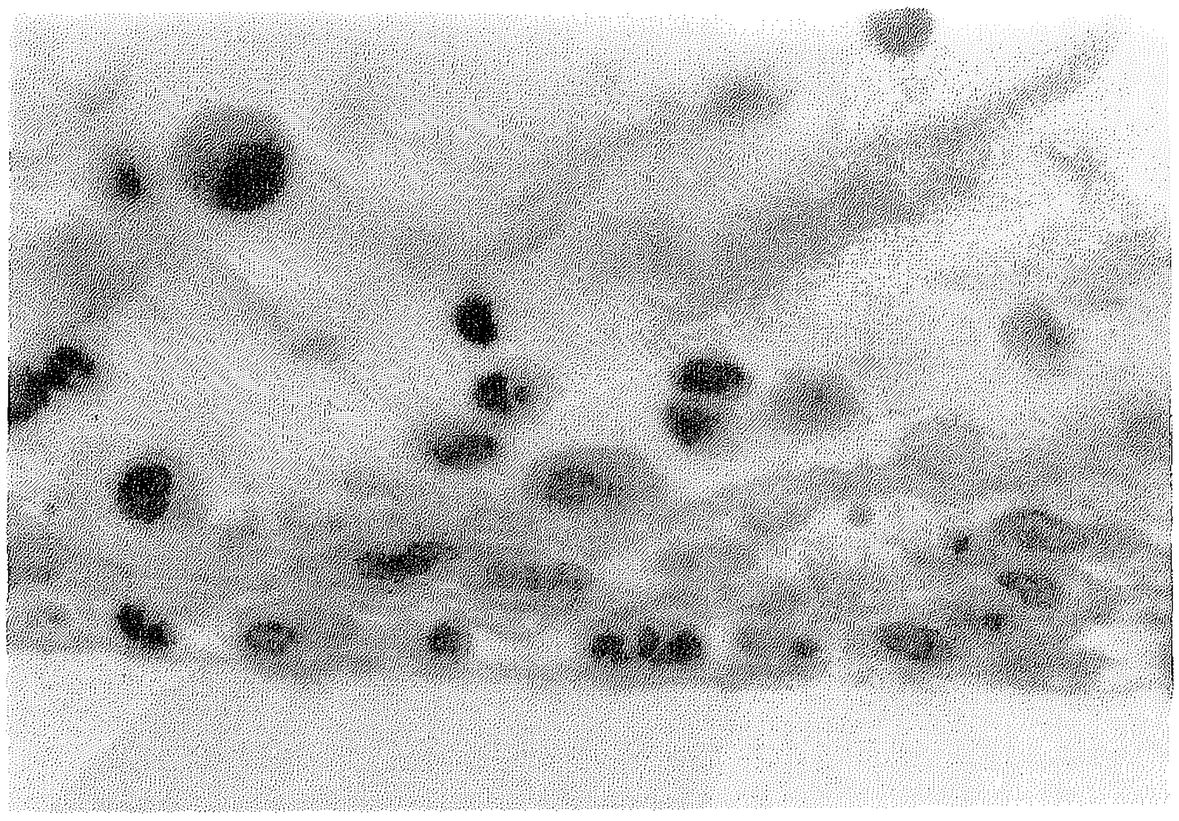

Figure 6. Detail of the accumulation of inflammatory cells at the interface after 3 days of implantation (10.0 μm implant; HE stain; original magnification 400×).

The histological appearance of the tissues after the 42 and 84 day implantation periods was highly comparable. For both implantation periods, the implant surrounding capsules were seen to consist of tightly packed, mature collagen. Embedded in this matrix, flat elongated fibroblasts were observed. At the interface between the tissues and the lumen of the removed implant flattened fibroblasts, but no inflammatory cells, were seen (Fig. 10).

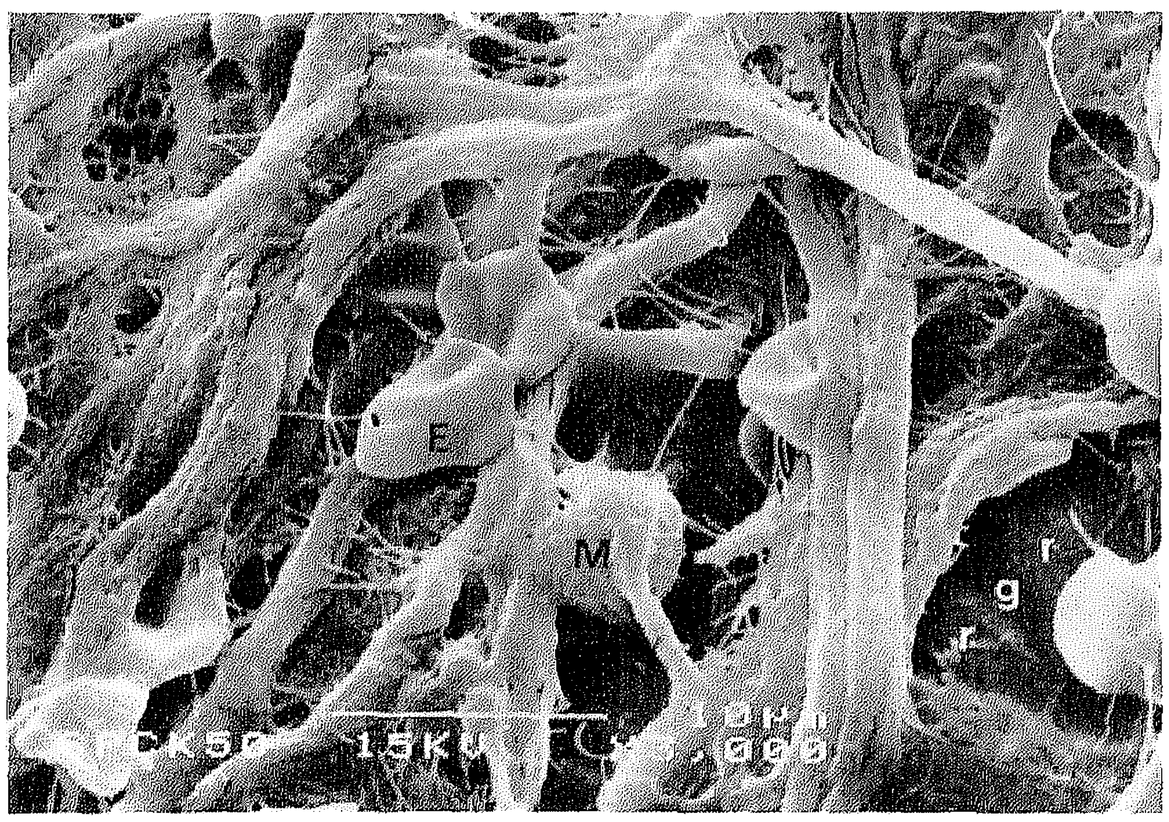

Figure 5. On this SEM image (3 days of implantation), the 2.0 μm grooved silicone surface (G = groove, R = ridge) is visible underneath the collagen fibers. Several punctured erythrocytes (E) and a macrophage (M) are located within the collagen matrix.

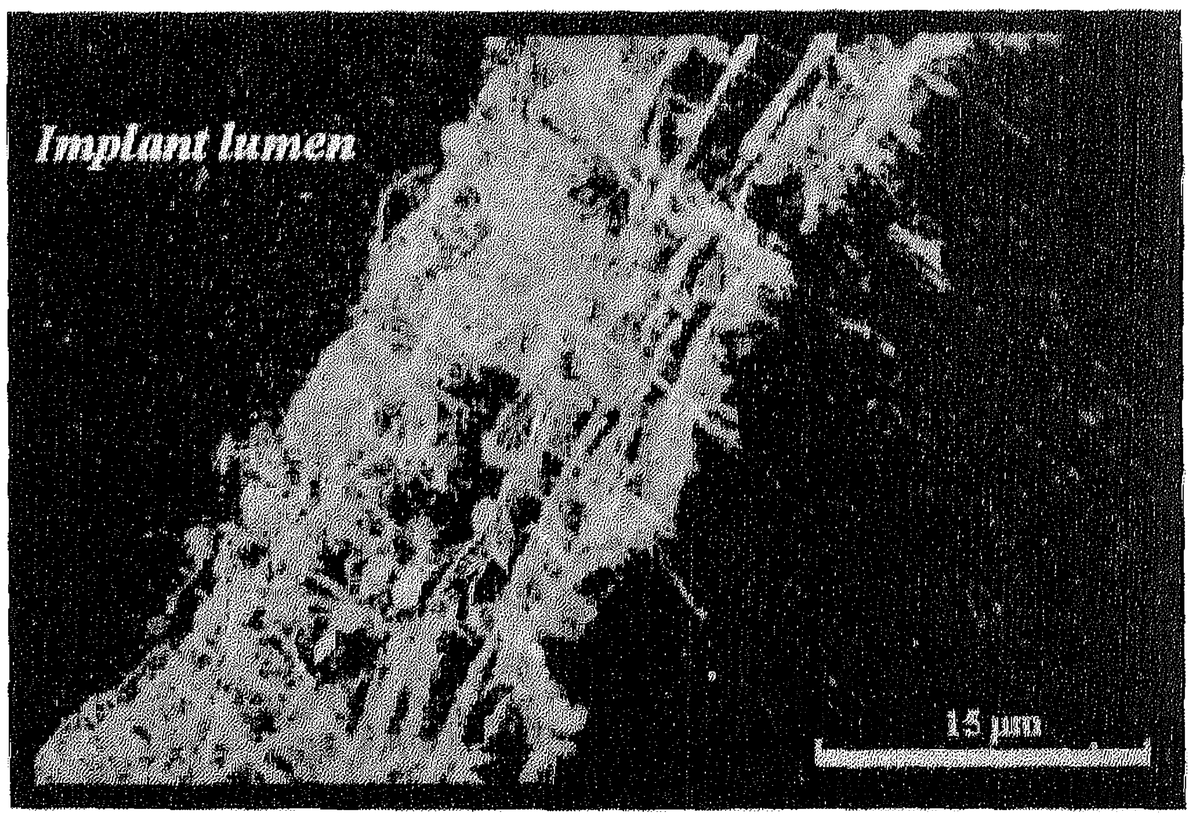

Figure 7. Three-dimensional reconstructed CLSM image of the collagen fibers in the implant surrounding capsule after 3 days of implantation (5.0 μm implant). The collagen fibers are oriented parallel and perpendicular to the implant surface. In addition, small globular collagen concentrations can be seen.

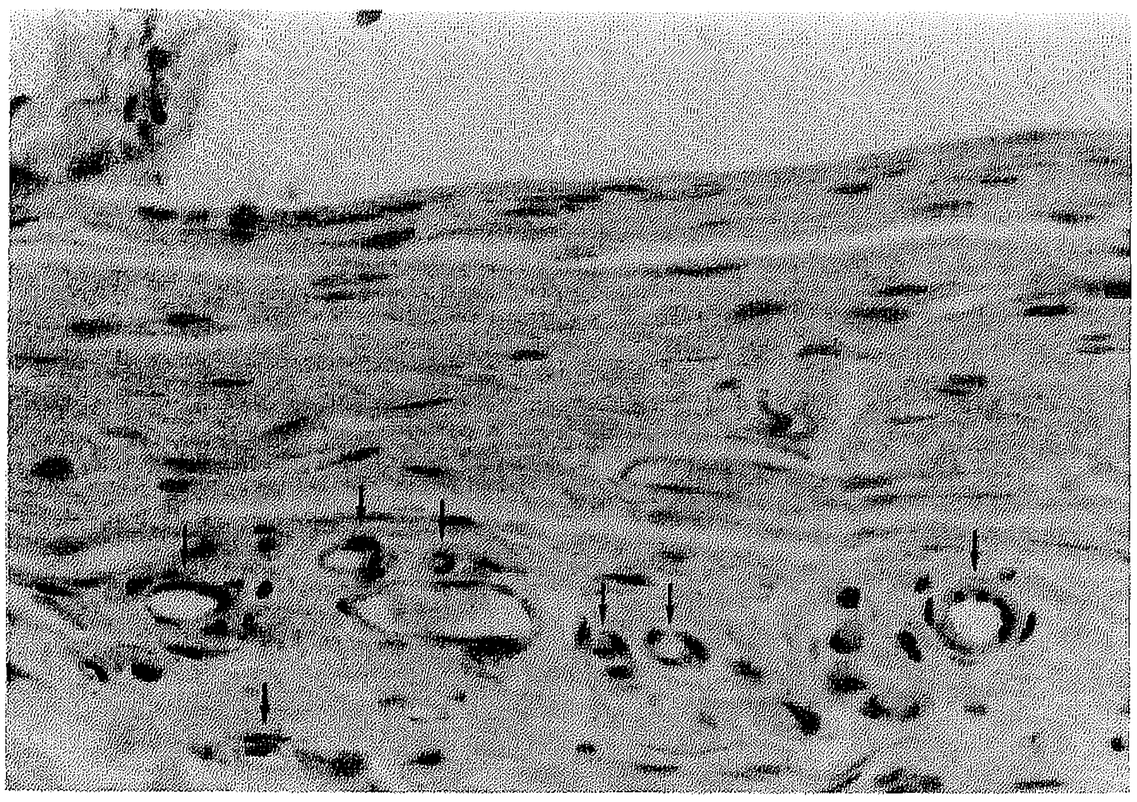

Figure 8. After 7 days of implantation many blood vessels (arrows) can be seen in the capsule. The more tightly packed capsule possessed several layers of flattened fibroblasts (2.0 μm implant, original magnification 160×).

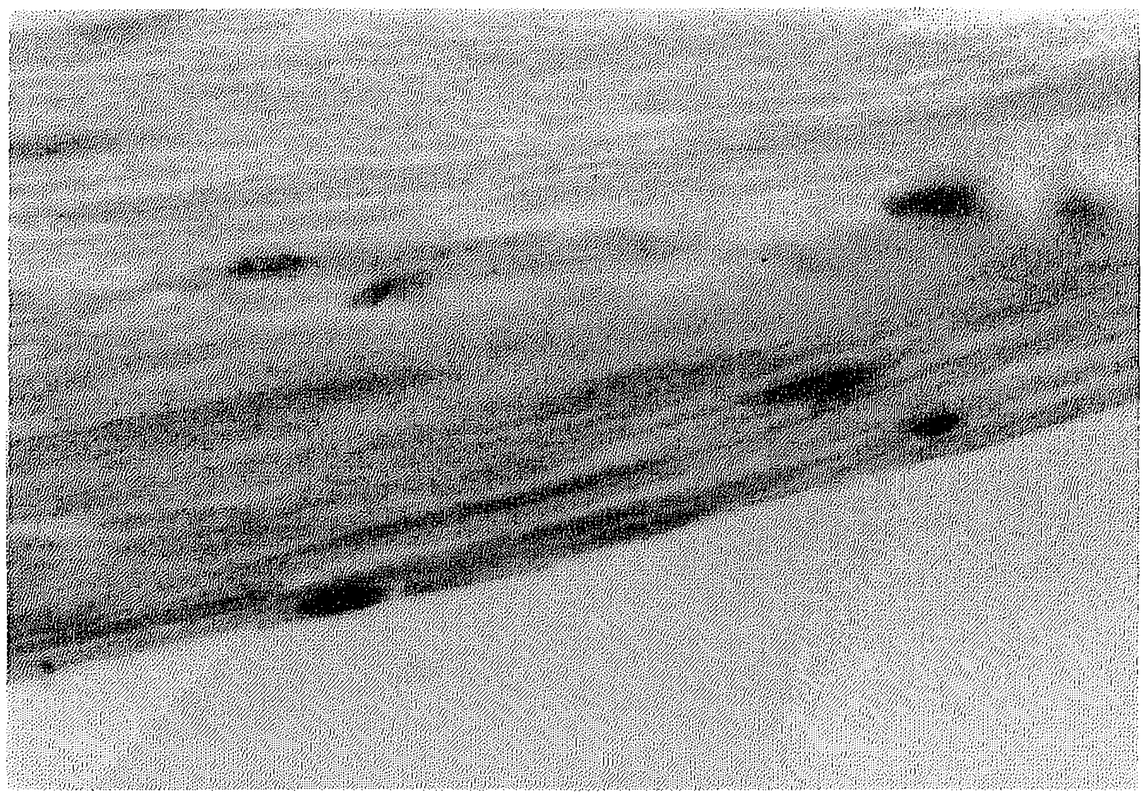

Figure 10. High magnification of the fibroblasts at the interface of capsule and the implant lumen after 84 days of implantation. The fibroblasts are flattened and arranged parallel to the implant surface. No inflammatory cells are present (5.0 μm implant; Mason Trichrome stain; original magnification 400×).

Histomorphometric evaluation of the tissues surrounding the implant

Statistical analysis with the Spearman correlation model showed that there is no correlation between the location of a specific implant type (Fig. 1) and the values of the investigated parameters (Table II) for each of the implantation periods ($0.10052 \leqslant r_s \leqslant 0.31569$). However, high correlation was found when parameter scores were compared for the same evaluation fields (Fig. 2) of identically textured implants within a single implantation period ($0.88941 \leqslant r_s \leqslant 0.96923$). In contrast, the correlation between fields 10 to 15 (smooth-side implant) of different textured implants within a single implantation period proved to be relatively low ($0.19560 \leqslant r_s \leqslant 0.37317$).

Statistical evaluation of parameters mentioned in Table II with a Fisher Exact test showed that the capsules surrounding all implants became significantly more dense with increasing length of the implantation period ($2.17 \times 10^{-5} \leqslant P_{3\text{–}84\ \text{days}} \leqslant 0.0241$). Furthermore, the thickness of this capsule, measured by counting the layers of fibroblasts, proved to increase significantly over time ($7.36 \times 10^{-8} \leqslant P_{3\text{–}84\ \text{days}} \leqslant 0.0054$). On the other hand, no significant differences in capsule density or thickness were detected between the smooth and the textured implant surfaces for all implants during all implantation periods (Fig. 11). In contrast, differences were found for the number of inflammatory cells that were present at the interface between the implant lumen and the surrounding tissues (Fig. 12). It proved that after an implantation period of 42 and 84 days, significantly more inflamma-

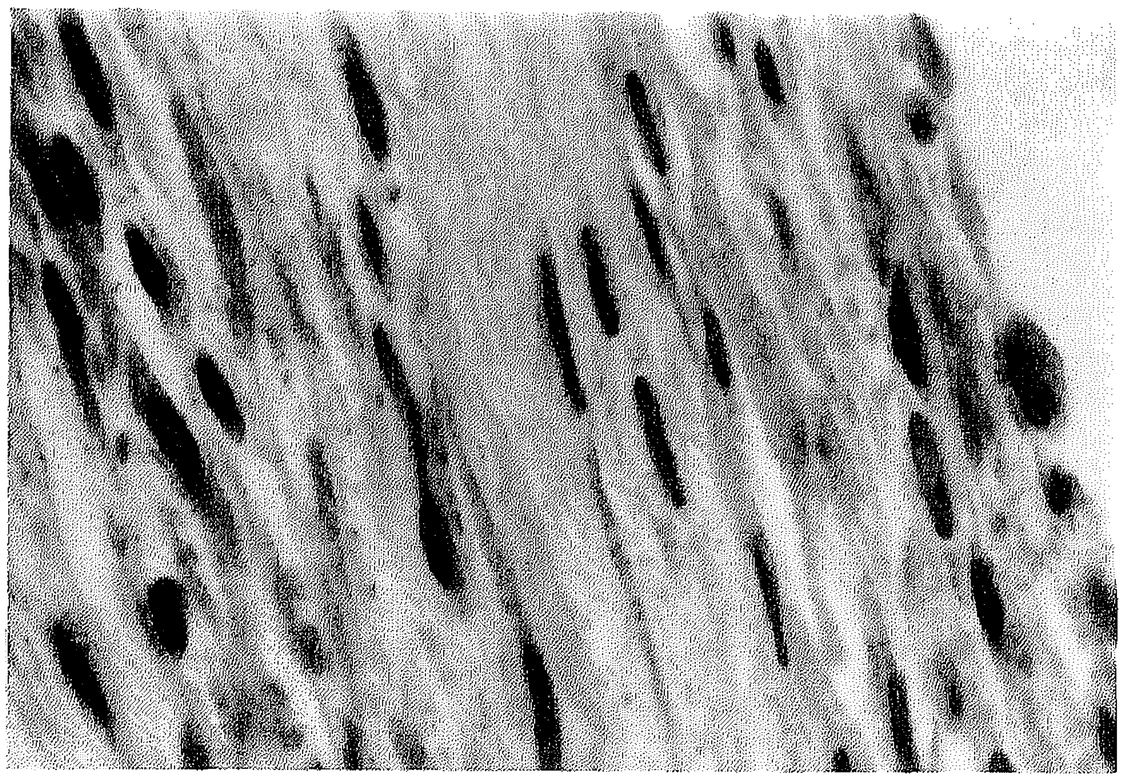

Figure 9. Magnification shows the decrease of the number of inflammatory cells at the interface and the various nucleus shapes of the fibroblasts in the capsule after 7 days of implantation (2.0 μm implant; Mason Trichrome stain; original magnification 400×).

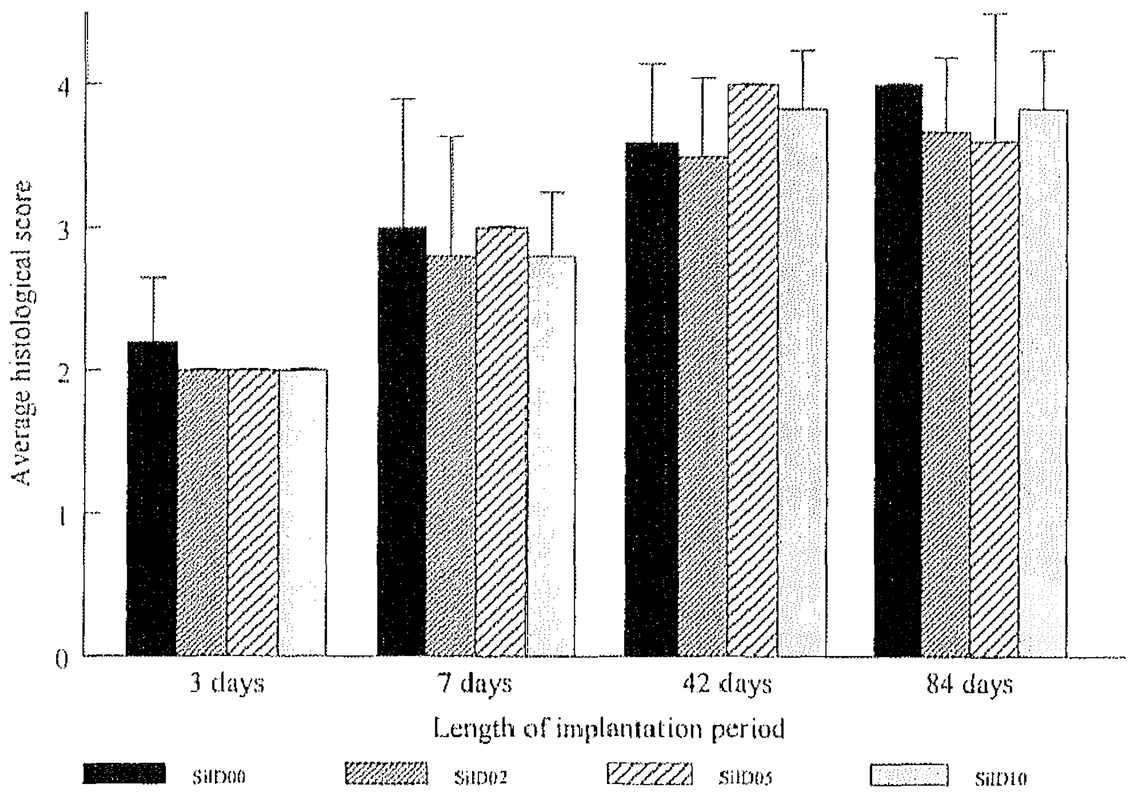

Figure 11. Average histological scores for capsule thickness (Table II). No significant differences were detected among the various textured implants with identical implantation periods.

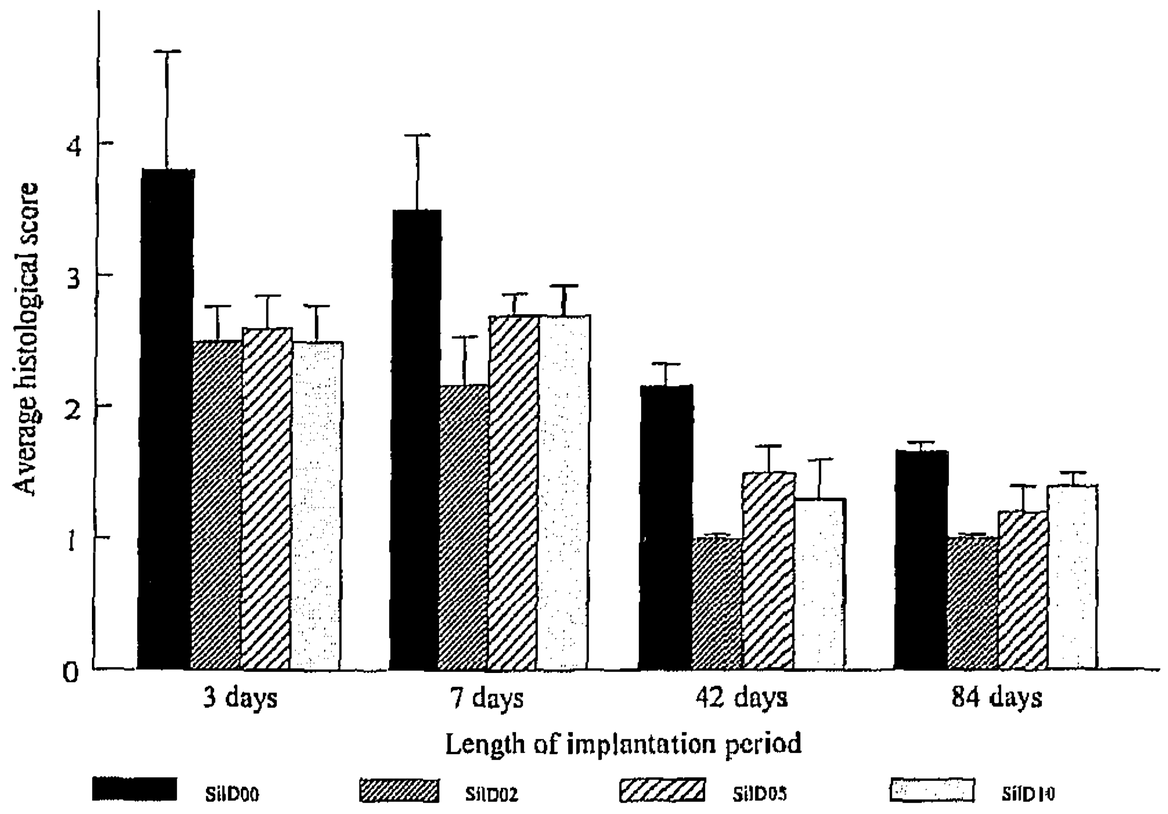

Figure 12. Average histological scores for the severity of the inflammatory process (Table II). Significant differences were detected between the smooth and the textured implants for all implantation periods.

tory cells ($0.0018 \leqslant P \leqslant 0.026$) were present at the interface with the SilD00 implant lumen than at the SilD02, SilD05, and SilD10 implant lumen interfaces. No significant differences in the number of inflammatory cells were detected between the smooth and textured sides of the SilD02, SilD05, and SilD10 implants. Moreover, significantly more inflammatory cells were present in the SilD00 implant capsules than in the SilD02, SilD05, and SilD10 implant capsules during all the incubation periods ($0.00625 \leqslant P_{3\text{–}84\ \text{days}} \leqslant 0.0158$). During these implantation periods it was found that the various types of inflammatory cells in the tissues surrounding the smooth and textured implants did not differ ($P_{3\text{–}84\ \text{days}} \geqslant 0.122$). Finally, no significant differences concerning the presence, position, or type of inflammatory cells were found for the SilD02, SilD05, and SilD10 implants ($P_{3\text{–}84}$ days $\geqslant 0.211$).

For the presence and location of blood vessels, it was found that the number of vessels that were present in the capsules of all the implants did differ significantly. After 7 days of implantation, small vessels were present in the capsule of all implants. Statistical testing showed that the number of vessels in the capsule was significantly lower with the SilD00 implants than with the SilD02, SilD05, and SilD10 implants ($0.00293 \leqslant P_{7\text{–}84\ \text{days}} \leqslant 0.0272$). No significant differences in the number of vessels were detected among the SilD02, SilD05, and SilD10 implants nor between the textured and smooth sides of these implants. Finally, the number of vessels that was observed in the capsule of all the implants was the highest after 7 days of implantation, and significantly decreased with longer implantation periods ($P \leqslant 0.0469$).

DISCUSSION AND CONCLUSIONS

The results of this study did not show significant differences in capsule thickness between smooth and textured implant surfaces (Fig. 11). Although the CLSM images made it possible to observe the development of the collagen matrix in the capsule over time, no differences could be detected that might have been caused by the texture of the implant surfaces. In addition, the histological evaluation combined with the statistical analysis showed that after 84 days of implantation the capsules surrounding all implants were at least 20 fibroblasts thick. These findings do not support the hypothesis that microtextured implant surfaces reduce the size of the capsule surrounding these implants.[1,2] According to this hypothesis, the size of the capsule is reduced by a mechanical interlocking between the implant and the surrounding tissues. The interlocking would reduce the stress and movement at the implant interface and limit the consequential "mechanical irritation" of the surrounding tissues, which is supposed to induce tissue damage, fibrosis, and severe inflammatory responses.[1,2,7,8] Other investigators, indeed, have reported reduction of the capsule size due to microtextured surfaces. However, review of these studies[7,8,22,23] shows that the surface texture of the implants in these studies differs significantly from our implants, both in terms of microfeature appearance (pores, pillars, tapered pits, or V-shaped grooves) and dimensions (feature depth, size, and pitch). These considerable differences make it possible to suggest that the dimensions of our grooves and ridges were not sufficient to facilitate mechanical interlocking. As a result, the "mechanical irritation" of the smooth and grooved surfaces would be comparable, resulting in capsules of equal thickness. Furthermore, our textured implants possessed one smooth and one textured side. Although this opened up the possibility for intra-implant evaluation, it did not enhance possible mechanical interlocking between the implant and the surrounding tissues. Therefore, it can be questioned whether the capsule thickness would have been less if both sides of the implant had been textured.

Considering the results found for the capsule thickness, it is remarkable that significantly more inflammatory cells were present in the smooth implant capsules than in the capsule surrounding the textured implants (Fig. 12). In addition, it is surprising that these differences were not found between the smooth and textured sides of the SilD02, SilD05, and SilD10 implants. This suggests that the influence of the textured implant surface on the surrounding tissue transcends the area directly in contact with these surfaces. Several hypotheses apply as possible explanations for the observed discrepancies. For instance, it is suggested that mechanical interlocking could reduce the interfacial shear forces, which are supposed to induce severe inflammatory responses. However, considering the thickness of the capsule surrounding the implant, it remains doubtful whether mechanical interlocking

did occur. Another possibility could be that direct attachment of fibroblasts to the implant surface promotes implant immobilization and therefore prevents or diminishes the presence of inflammatory cells at the implant/tissue interface.[5] That fibroblasts attach to the implants was observed with SEM, while LM showed that fibroblasts were present at the interface between tissues and implant lumen after prolonged implantation (Fig. 10). The question remains, however, whether or not this direct attachment of fibroblasts to the implant surface is strong and durable enough to induce the observed differences in inflammatory response.

Our SEM observations also showed that the fibroblasts on the textured implant surfaces did not orient themselves parallel to the surface grooves. This is not in agreement with the findings of earlier *in vitro* studies.[1,2,4,16,18,24–26] In addition, our previous CLSM study[20] with RDFs on microtextured surfaces showed that intracellular components were aligned along SilD02 grooves and ridges. A possible explanation for these differences between *in vitro* and *in vivo* orientational cell behavior could be that the cells that are used in *in vitro* studies are isolated cells, cells that have no contact with other cells, cell types, or ECM. Previous studies[4,24,25] show that prolonged *in vitro* incubation on microtextured surfaces results in the formation of cell–cell contacts, an increase of the spread area, and a decrease of the orientation of the cells on these surfaces. Consequently, it was supposed that the observed guidance phenomenon is an initial response of cells *in vitro* to certain microtextured surfaces, which gradually is lost after cell–cell contacts are formed.[4,24,25] In tissues, these contacts with other cells are already present, which could mean that the orientational effect of the textured surfaces is overruled by stronger tissue-related signals or cues.

Concerning the vascularity of the capsules, we observed that significantly more blood vessels were present in the capsules of the microgrooved implants after 7 days of implantation. Although other studies[8,24] also reported a higher incidence of blood vessels in the capsules surrounding textured implants, the validity of a comparison can be questioned. Indeed, in both studies microtextured silicone rubber implants were used, but the textures of the surfaces were considerably different. In one study,[27] an aspecific, noncharacterized, rough surface was used while in the other[8] a pillared surface was implanted with pillars 10,000 times higher than the ridges in this study. Furthermore, the latter reports only an improved blood vessel proximity and does not issue any statements on the origin or status of these vessels. In our study, the observed vessels after 7 days of implantation appeared to be newly formed, but their numbers decreased with longer implantation periods. This could indicate that the formation and presence of these vessels were part of the proliferation phase of the wound healing process.[28,29] This proliferation phase is a part of the formation of granulation tissue, which is characterized by high fibroblast densities, the formation of new blood vessels, and a new connective tissue matrix.[28,29] After repair, the number of the vessels generally decreases, marking the end of the wound healing process and the start of a steady state. The fact that more vessels were observed around the textured implants during our study could indicate a higher rate of tissue repair.

In conclusion, it can be said that our study did not show any changes in thickness of the capsule surrounding the implant due to the shallow implant surface grooves. As mentioned before, deeper grooves perhaps could improve the mechanical interlocking between the tissues and the implant, thereby reducing the thickness of the capsule. If such a reduction could be achieved, this would enhance the performance of many soft-tissue implants. In addition, differences were observed in inflammatory response and in the number of blood vessels. Further research perhaps could clarify what mechanisms cause these phenomena and whether the observed differences change if the depth of the surface grooves increases.

The authors would like to thank Professor A. F. von Recum (Clemson University, USA) for the microtextured silicon wafers that were produced under his supervision. In addition, the help of Dr. P. H. K. Jap and H. A. L. van der Lee with the histological staining procedures was greatly appreciated.

References

1. A. F. von Recum and T. G. van Kooten, "The influence of micro-topography on cellular response and the implications for silicone implants," *J. Biomater. Sci. Polym. Ed.*, **7**, 181–198 (1995).
2. R. Singhvi, G. Stephanopoulos, and D. I. C. Wang, "Review: Effects of substratum morphology on cell physiology," *Biotech. Bioeng.*, **43**, 764–771 (1994).
3. B. D. Ratner, "New ideas in biomaterial science—A path to engineered biomaterials," *J. Biomed. Mater. Res.*, **27**, 837–850 (1993).
4. A. S. G. Curtis and P. Clark, "The effects of topographic and mechanical properties of materials on cell behavior," *Crit. Rev. Biocompat.*, **5**, 344–362 (1990).
5. B. Chehroudi, T. R. Gould, and D. M. Brunette, "Effects of a grooved epoxy substratum on epithelial cell behavior *in vitro* and *in vivo*," *J. Biomed. Mater. Res.*, **22**, 459–473 (1988).
6. B. Chehroudi, T. R. L. Gould, and D. M. Brunette, "A light and electron microscope study of the effects of surface topography on the behavior of cells attached to titanium-coated percutaneous implants," *J. Biomed. Mater. Res.*, **25**, 387–405 (1991).
7. C. E. Campbell and A. F. von Recum, "Microtopography and soft tissue response," *J. Invest. Surg.*, **2**, 51–74 (1989).
8. G. J. Picha and R. F. Drake, "Pillared-surface micro-

structure and soft-tissue implants: Effect of implant site and fixation," *J. Biomed. Mater. Res.*, **30,** 305–312 (1996).
9. J. A. Jansen and K. de Groot, "Guinea pig and rabbit model for the histological evaluation of permanent percutaneous implants," *Biomaterials*, **9**, 268–272 (1988).
10. J. A. Jansen, J. P. C. M. van der Waerden, H. B. M. van der Lubbe, and K. de Groot, "Tissue response to percutaneous implants in rabbits," *J. Biomed. Mater. Res.*, **24**, 295–307 (1990).
11. J. A. Jansen, "Development of a new percutaneous access device for implantation in soft tissues," *J. Biomed. Mater. Res.*, **25**, 1535–1545 (1991).
12. J. A. Jansen, J. P. C. M. van der Waerden, and K. de Groot, "Fibroblast and epithelial cell interactions with surface-treated implant materials," *Biomaterials*, **12**, 25–31 (1991).
13. J. A. Jansen, E. T. den Braber, and Y. Paquay, "Percutaneous implants," in *Materials in Clinical Applications: Advances in Science and Technology*, **12**, P. Vincenzini (ed.), Techna, Faenza, Italy, 1995, pp. 779–790.
14. J. A. Schmidt and A. F. von Recum, "Texturing of polymer surfaces at the cellular level," *Biomaterials*, **12**, 385–389 (1991).
15. J. A. Schmidt and A. F. von Recum, "Surface characterization of microtextured silicone," *Biomaterials*, **13**, 675–681 (1992).
16. E. T. den Braber, J. E. de Ruijter, H. T. J. Smits, L. A. Ginsel, A. F. von Recum, and J. A. Jansen, "Quantitative analysis of fibroblast morphology on microgrooved surfaces with various groove and ridge dimensions," *Biomaterials*, **17**, 2037–2044 (1996).
17. J. A. Jansen and M. A. van't Hof, "Histological assessment of sintered metal–fiber–web materials," *J. Biomater. Appl.*, **9**, 30–54 (1994).
18. E. T. den Braber, J. E. de Ruijter, H. T. J. Smits, L. A. Ginsel, A. F. von Recum, and J. A. Jansen, "Effect of parallel surface microgrooves and surface energy on cell growth," *J. Biomed. Mater. Res.*, **29**, 511–518 (1995).
19. L. Vacca, *Laboratory Manual of Histochemistry*, Raven Press Ltd., New York, 1985.
20. E. T. den Braber, J. E. de Ruijter, L. A. Ginsel, A. F. von Recum, and J. A. Jansen, "Confocal laser scanning microscopical study of the cytoskeletal architecture, attachment complexes, and protein depositions of fibroblasts cultured on silicone microgrooved surfaces," *J. Biomed. Mater. Res.*, submitted.
21. J. A. Jansen, W. J. A. Dhert, J. P. C. M. van der Waerden, and A. F. von Recum, "Semi-quantitative and qualitative histologic analysis method for the evaluation of implant biocompatibility," *J. Invest. Surg.*, **7**, 123–134 (1994).
22. C. A. Squier and P. Collins, "The relationship between soft tissue attachment, epithelial downgrowth and surface porosity," *J. Periodont. Res.*, **16**, 434–440 (1981).
23. B. Chehroudi, T. R. Gould, and D. M. Brunette, "The role of connective tissue in inhibiting epithelial downgrowth on titanium-coated percutaneous devices," *J. Biomed. Mater. Res.*, **26**, 493–515 (1992).
24. P. Clark, P. Connolly, A. S. G. Curtis, J. A. T. Dow, and C. D. W. Wilkinson, "Cell guidance by ultrafine topography *in vitro*," *J. Cell Sci.*, **99**, 73–77 (1991).
25. E. T. den Braber, J. E. de Ruijter, H. T. J. Smits, L. A. Ginsel, A. F. von Recum, and J. A. Jansen, "Quantitative analysis of cell proliferation and orientation on substrata with uniform parallel surface micro-grooves," *Biomaterials*, **17**, 1093–1099 (1996).
26. B. Chehroudi and D. M. Brunette, "Effects of surface topography on cell behavior," in *Encyclopedic Handbook of Biomaterials and Bioengineering*, D. L. Wise, D. J. Trantolo, D. E. Altobelli, M. J. Yaszemski, J. D. Gresser, and E. R. Schwartz (eds.), Marcel Dekker Inc., New York, 1995, pp. 813–842.
27. S. Bern, A. Burd, and J. May, Jr., "The biophysical and histologic properties of capsules formed by smooth and textured silicone implants in the rabbit," *Plast. Reconstr. Surg.*, **89**, 1037–1042 (1992).
28. A. F. von Recum, H. Opitz, and E. Wu, "Collagen types I and III at the implant/tissue interface," *J. Biomed. Mater. Res.*, **27**, 757–761 (1993).
29. H. P. Ehrlich, "Regulation der Wundheilung aus der Sicht des Bindesgewebes," *Der Chirurg*, **66**, 165–173 (1995).